



AUSTRALIAN ATOMIC ENERGY COMMISSION
RESEARCH ESTABLISHMENT
LUCAS HEIGHTS

STUDIES OF THE EFFECT OF THICKNESS ON THE FRACTURE
TOUGHNESS OF GRADE 300 MARAGING STEEL, PART 1

by

P.D. SMITH
K.R. BROWN

June 1977

ISBN 0 642 99786 1

AUSTRALIAN ATOMIC ENERGY COMMISSION
RESEARCH ESTABLISHMENT
LUCAS HEIGHTS

STUDIES OF THE EFFECT OF THICKNESS ON THE FRACTURE
TOUGHNESS OF GRADE 300 MARAGING STEEL, PART 1

by

P.D. SMITH
K. BROWN

ABSTRACT

A series of tests was carried out using the ASTM fracture toughness test standards as a basis to determine the variation in fracture toughness of maraging steel (grade 300) of thickness ranging from 10 to 1 mm. Although these standards are not strictly applicable to maraging steels of the lower thicknesses in this range, they yield a measure of fracture toughness which can be used to predict safe operating stresses for thin walled structures. A maximum fracture toughness of approximately $90 \text{ MPa m}^{\frac{1}{2}}$ was obtained at 1 mm, the minimum thickness examined. The plane strain fracture toughness was approximately $58 \text{ MPa m}^{\frac{1}{2}}$ at thicknesses greater than 5 mm.

National Library of Australia card number and ISBN 0 642 99786 1

The following descriptors have been selected from the INIS Thesaurus to describe the subject content of this report for information retrieval purposes. For further details please refer to IAEA-INIS-12(INIS: Manual for Indexing) and IAEA-INIS-13(INIS: Thesaurus) published in Vienna by the International Atomic Energy Agency.

FRACTURE PROPERTIES; THICKNESS; MARAGING STEELS; SHEETS

CONTENTS

	<u>Page</u>
1. INTRODUCTION	1
2. EXPERIMENTAL DETAILS	1
3. RESULTS	3
4. DISCUSSION	4
5. CONCLUSIONS	6
6. REFERENCES	6
Table 1	Nominal Commercial Analysis
Table 2	Fracture Toughness Values
Table 3	Critical Crack Sizes for Through-Wall Cracks
Figure 1	Fracture toughness test specimen
Figure 2	Loading system showing detachable knife edges used to hold the clip gauge extensometer
Figure 3	Plot of fracture toughness, K_q , against specimen thickness
Figure 4	SEM fractograph showing outer shear lips and central plane strain region on 1 mm thick specimen. Fatigue crack on left. Magnification X 90.
Figure 5	SEM fractograph showing shear lip at bottom and fatigue crack on left of 5 mm thick specimen. Magnification X 60.
Figure 6	SEM fractograph showing ductile nature of central plane strain region of 5 mm thick specimen. Magnification X 1000.
Figure 7	Variation of fracture toughness with sheet thickness predicted by the models of Bluhm [1961].
Figure 8	Critical flaw size for structures of varying thickness at a stress of 0.85 of the yield stress.

1. INTRODUCTION

Maraging steels are candidate materials for use in highly stressed lightweight structures. For these applications they must have high strength, high creep resistance to prevent distortion during service, good corrosion and stress corrosion resistance in the environments encountered in service, and they must have high fracture toughness. For weight and economy, the structural section should be a minimum, but little is known of the fracture properties of thin sections of maraging steel.

It is known that thin sections of many materials [Brown & Strawley 1966; Sullivan, Stoop & Freed 1973] exhibit better fracture toughness than the same material in thicker sections. The series of tests reported here was designed to establish the effect of thickness on the fracture toughness of 18% nickel maraging steel, grade 300.

ASTM standards for the determination of the fracture toughness of a material [ASTM 1974] are only valid on materials that have a section large enough to ensure that plane strain conditions prevail. To meet ASTM requirements the specimen thickness must exceed the parameter

$2.5 \left[\frac{K_{1c}}{\sigma_{ys}} \right]^2$; however we believe that the fracture toughness value measured on a specimen of a certain thickness can be applied to the use of that material in that section. The plane strain fracture toughness may be unduly pessimistic when applied to the material in thin sections in a highly stressed component.

2. EXPERIMENTAL DETAILS

The material used was commercial grade 300 maraging steel of the nominal analysis shown in Table 1. Charpy specimens were cut from 100 mm diameter forged bar such that the axis of the notch was parallel to the axis of the bar. Specimens for notched three-point bend tests were machined from standard Charpy test specimens as shown in Figure 1. The test thickness was varied by machining away the surfaces of the specimen (Figure 1). Before the final machining, the Charpy specimens were solution heat treated in argon at 816°C for 1 hour.

A fatigue crack was then grown approximately 1 mm from the notch by loading the sample on a three-point bend fatigue cracking machine. This machine, designed and made at the AAEC, consists of an electric motor which drives a heavy duty ball bearing on an eccentric shaft. The ball bearing provides the centre loading of the three-point bend and the specimen is loaded against it by a screw thread on the specimen holder.

The output from a strain gauge bridge attached to the specimen holder had been previously calibrated in terms of load, and its output during fatigue cracking was observed on an oscilloscope.

During load cycling a microscope was used to provide continuous observation of the notched area on the specimen. When the crack had grown to the desired length the load was removed from the specimen holder and the sample removed.

The fatigue cracks were nominally 1 mm in length but varied from 0.75 mm to 1.3 mm.

The maximum stress intensity during fatigue cycling was maintained at $0.7 K_{1c}$. Although the current ASTM limits require that the maximum stress intensity reached during fatigue cycling does not exceed $0.6 K_{1c}$, May [1970] reported that for maraging steel, stress intensities of up to $0.9 K_{1c}$ had no effect on the value of K_{1c} measured subsequently.

When required, the cross section of the specimen was reduced after the fatigue crack had been initiated, but before the sample was aged. This minimised machining difficulties and also removed the crack end-effects, thus reducing the curvature of the crack front.

After fatigue cracking and machining, the specimen was aged for 3 hours at 482°C in argon and then allowed to cool in air to room temperature.

According to ASTM standards the fatigue crack should have been inserted after machining and aging. However, attempts to fatigue crack the material in the fully aged condition were unsuccessful. The peak load that was required to initiate a fatigue crack in a reasonable time (less than 2 hours) was also sufficient to propagate the crack entirely across the specimen in only a few cycles of the fatigue loading. It was impossible to detect the crack and remove the load quickly enough to control the length of the crack accurately and consistently. In addition, when cracking in the heat-treated and aged condition small branch cracks would appear on and outside the plane of the initiating crack thus giving several starter cracks. Japanese workers have reported that this type of crack branching can give abnormally high and erroneous values of K_{1c} during subsequent testing [Kawabe et al. 1976].

The precracked and aged specimen was then tested under three-point load in a Tinius Olsen Universal testing machine at a loading rate of $8.5 \times 10^{-3} \text{ mm s}^{-1}$. A separate external load cell was used to record the load and a small clip gauge was attached to register the opening of the notch, Figure 2. The load and crack opening was recorded on an X-Y

recorder, and the curves analysed in accordance with ASTM E399-74.

Since our experimental conditions did not meet ASTM standards, particularly in relation to sample dimensions, we shall denote fracture toughness by K_q , the ASTM designation for provisional fracture toughness. The K_q in $\text{MPa m}^{1/2}$ for each specimen was calculated using the formula

$$K_q = (P_q S / BW^{3/2}) [2.9 (A/W)^{1/2} - 4.6 (A/W)^{3/2} + 21.8 (A/W)^{5/2} - 37.6 (A/W)^{7/2} + 38.7 (A/W)^{9/2}] \quad \dots (1)$$

- P_q = load (MPa)
 B = thickness of specimen (metres)
 S = span length (metres)
 W = specimen depth (metres)
 A = crack length (metres).

3. RESULTS

The results of the fracture toughness tests on specimens of varying thicknesses are shown in Table 2 and Figure 3. For duplicate tests on the 10 mm thick specimens the fracture toughness was found to be $60 \text{ MPa m}^{1/2}$, and for 5 mm thick specimens, $56 \text{ MPa m}^{1/2}$. This difference between 5 mm and 10 mm thick samples is thought attributable to experimental scatter, in which case an average value of $58 \text{ MPa m}^{1/2}$ for both sets of samples approximates the plane strain fracture toughness of the material. These tests complied with ASTM requirements for specimen thickness and notch acuity, and the results lie within the range of K_{1C} values reported by other workers for commercial grade 300 maraging steels [Kobe Steel Ltd 1975]. K_q increased with decreasing thickness; the highest K_q value for duplicate specimens averaged $91 \text{ MPa m}^{1/2}$ and was obtained for nominal sample thicknesses of 1 mm, the minimum thickness tested.

The fractography of all samples in the range 1 to 10 mm was similar. The central section of each sample consisted of a flat fracture face, resulting presumably from plane strain conditions, and on either side were shear lips 0.4 mm wide. The only obvious difference between the thinner and the thicker samples was in the relative proportion of shear lip to plane strain fracture. The width of the shear lips was approximately constant from the thinnest to the thickest sample (Figures 4 and 5). Both the central flat fracture (Figure 6), and the surface of the shear lips consisted

of dimples resulting from ductile tearing, and no areas of brittle cleavage failure were observed. Some inclusions were evident. This fractography is typical of maraging grade 300 steels and has been reported by most workers in the field. The fractographs agree well with those documented in the Metals Handbook Vol. 9, Fractography and Atlas of Fractographs [ASM 1974].

4. DISCUSSION

It would appear that the fracture toughness of maraging grade 300 steels may increase by 50% as the thickness is decreased from 5 to 1 mm. At thicknesses greater than 5 mm, plane strain conditions prevail and the fracture surface is flat. Below 5 mm the contribution of the antiplane strain shear lips becomes relatively greater, with the result that the fracture toughness increases markedly. In this region the fracture is by mixed mode, and is partially flat plane strain fracture and partially shear lips.

The width of the shear lips formed after the fracture had propagated ~1-2 mm remained relatively constant at 0.4 mm and was independent of thickness in the range examined. At 0.8 mm thickness, the shear lips might occupy all of the fracture surface to correspond with the maximum value of K_I [Duke & Brown 1977]. It would be expected that as the thickness decreased still further, K_I would remain constant or begin to decrease as the size of inclusions or defects within the sheet became significant in relation to the sheet thickness. The same behaviour has been observed by others, in maraging steels [Knott 1973] and aluminium [Sullivan, Stoop & Freed 1973].

These results may be compared with the empirical model of Bluhm [1961] and Krafft, Sullivan & Boyle [1961] who relate fracture toughness and thickness by

$$g_c = \frac{1}{2} k_{SL} B_{SL_0} \left[\frac{B}{B_{SL_0}} \right]; \left[\frac{B}{B_{SL_0}} \right] < 1 \quad \dots (2)$$

$$g_c = \frac{1}{2} k_{SL} B_{SL_0} \left[\frac{B_{SL_0}}{B} \right] + k_{ff} \left[1 - \frac{B_{SL_0}}{B} \right]; \frac{B}{B_{SL_0}} > 1 \quad \dots (3)$$

where $g_c = K_c^2/E$,

B_{SL_0} = critical (constant) total shear lip thickness, (0.8 mm)

B = sheet thickness

k_{SL} and k_{ff} = material constants (subscripts SL and ff refer to shear lip and flat fracture, respectively) and

$$k_{ff} = g_{lc}.$$

This model accounts for the relative amount of shear failure on the fracture surface, and assumes that the width of the shear lips remains constant once the sheet thickness is sufficient to allow their full development.

The average width (0.4 mm), of each shear lip observed on test specimens ranging from 1 mm to 10 mm in thickness, and a plane strain fracture toughness K_{lc} of 58 MPa m^{1/2} were used in these models to give Figure 7. To derive the plane stress region of this plot, a maximum value of fracture toughness of 105 MPa m^{1/2} was selected at a sheet thickness of 0.8 mm, this value being that determined in concurrent work by Duke and Brown [1977].

The value of the shear lip width (0.4 mm) used in deriving Figure 7 is the constant value established after the crack had moved ~1-2 mm, but it is likely that the crack may not have moved this distance at the measured load from which the fracture toughness was determined. In this case thinner shear lips would have been present (see Figures 4 and 5), and a lower value of fracture toughness would have been calculated from the model. Crack staining during testing could be used in future studies to determine the appropriate value of the shear lip width to be used in the model.

It would appear that this model could be used successfully to predict the sheet thickness for optimum K_q , if not with sufficient accuracy for design purposes, at least with enough precision for the judicious selection of test specimens. The necessary data can be obtained from a minimum of two specimens.

The significance of this increase in fracture toughness in the vicinity of 1 mm thickness should be examined in relation to the design of lightweight structures. Of particular importance is the size of a critical defect. A critical defect is one which is just large enough to propagate catastrophically at a given stress level.

The length of critical cracks that completely penetrate the wall of a structure may be calculated from the fracture toughness (Table 3, Figure 8); it can be seen that the critical size for through flaws at a stress of $0.85 \sigma_y$ approximately doubles as the thickness is reduced from 10 to 1 mm.

However, it would be expected that extraneous partial thickness flaws, such as those resulting from machining or accidental scratches from handling, would be more likely than through-thickness flaws. These would have similar depths in thin walled or thick walled structures but in a thin walled structure a defect of a specific depth is relatively more severe.

As the wall thickness is decreased from 10 mm to 1 mm the relative depth of a specific flaw increases, and it would be expected that the length, and hence the surface area, of a critical flaw would decrease in proportion as shown in Figure 8. However, because of the increase in fracture toughness in this thickness range, the critical length and surface area of a flaw of a specific depth, decrease by a factor of only five in the thickness range 10 to 1 mm (Figure 8). It can be seen that for thicknesses in the range 2 to 5 mm, the critical size of flaws of a specific depth is approximately constant.

5. CONCLUSIONS

1. The fracture toughness of 300 grade maraging steel increases from approximately 58 to ~90 MPa m^{1/2} as the thickness decreases from 5 mm to 1 mm. Above 5 mm in thickness, plane strain conditions prevail and the test material was found to have a K_{1C} of approximately 58 MPa m^{1/2}.

2. Through this thickness range, the critical crack size for a through-wall flaw increases from ~0.8 mm to 2 mm at an operating stress of 1620 MPa which approximates 85% of the yield strength.

3. In the thickness range 10 to 1 mm, the critical length of flaws of a specific absolute depth decreases by a factor of five. Within the thickness range 2 to 5 mm, the critical size of these flaws is approximately constant.

6. REFERENCES

- ASM 'Metals Handbook Vol. 9, Fractography and Atlas of Fractographs', 1974. ASTM-E399-74, page 561. Plane Strain Fracture Toughness of Metallic Materials.
- Bluhm, J.I. [1961] - Proc. ASTM Vol. 61.
- Brown, W.F. & Strawley, J.E. [1966] - Plane strain crack toughness testing of high strength metallic materials. ASTM Special Technical Publication 410, ASTM p.1.
- Central Research Laboratories, Kobe Steel Ltd , Kobe, Japan, May 1975 - '18% Ni Maraging Steel.' Technical Report.

- Duke, C. & Brown, K.R. [1977] - 'Further Studies of the Effect of Thickness on the Fracture Toughness of Maraging Steel', AAEC/E406.
- Kawabe, Y., Nakazawa, K., Kanao, M. & Muneki, S. [1976] - Effects of the Aged Structure and the Prior Austenite Grain Size on Fracture Toughness of 18 Ni Maraging Steels' - National Research Institute for Metals, Tokyo, Japan.
- Knott, J.F. [1973] - 'Fundamentals of Fracture Mechanics', Butterworths, London, p.115.
- Krafft, J.M., Sullivan, A.M. & Boyle, R.W. [1961] - 'Effect of Dimensions on Fast Fracture Instability of Notched Sheet', Proc. Crack Propagation Symposium, Cranfield, U.K.
- May, M.J. [1970] - 'Review of Developments in Plane Strain Crack Toughness Testing of High Strength Metallic Materials', ASTM STP 463, p.42.
- Sullivan, A.M., Stoop, J. & Freed, C.N. [1973] - Influence of sheet thickness upon the fracture resistance of structural aluminium alloys. Progress in Flaw Growth and Fracture Toughness Testing, ASTM Special Technical Publication 536, ASTM p.323.

TABLE 1
NOMINAL COMMERCIAL ANALYSIS

C	Si	Mn	S	P	Ni	Co	Mo	Ti	Al
0.01	0.05	0.05	0.005	0.005	18.5	9.0	4.85	0.75	0.10

TABLE 2
FRACTURE TOUGHNESS VALUES

Specimen No.	Thickness (mm)	Crack Depth (mm)	Load (kg)	Fracture Toughness (MPa m ^{1/2})
3	10	3.046	802.87	61.6
7	10	3.046	771.10	59.2
4	5	3.35	328.40	54.5
8	5	3.046	370.14	56.9
5	2	2.792	202.30	72.8
9	2	3.299	229.07	94.0
6	1	2.792	118.84	85.5
10	1	2.792	135.17	97.2

TABLE 3
CRITICAL CRACK SIZES FOR THROUGH-WALL CRACKS
STRESS LEVEL 1620 MPa (0.85 σ_y)

Material Thickness (mm)	Fracture Toughness (MPa m ^{1/2})	Critical Crack Length (mm)
10	61.6	0.9
10	59.2	0.9
5	54.5	0.7
5	56.9	0.8
2	72.8	1.3
2	94.0	2.2
1	85.5	1.8
1	97.2	2.4

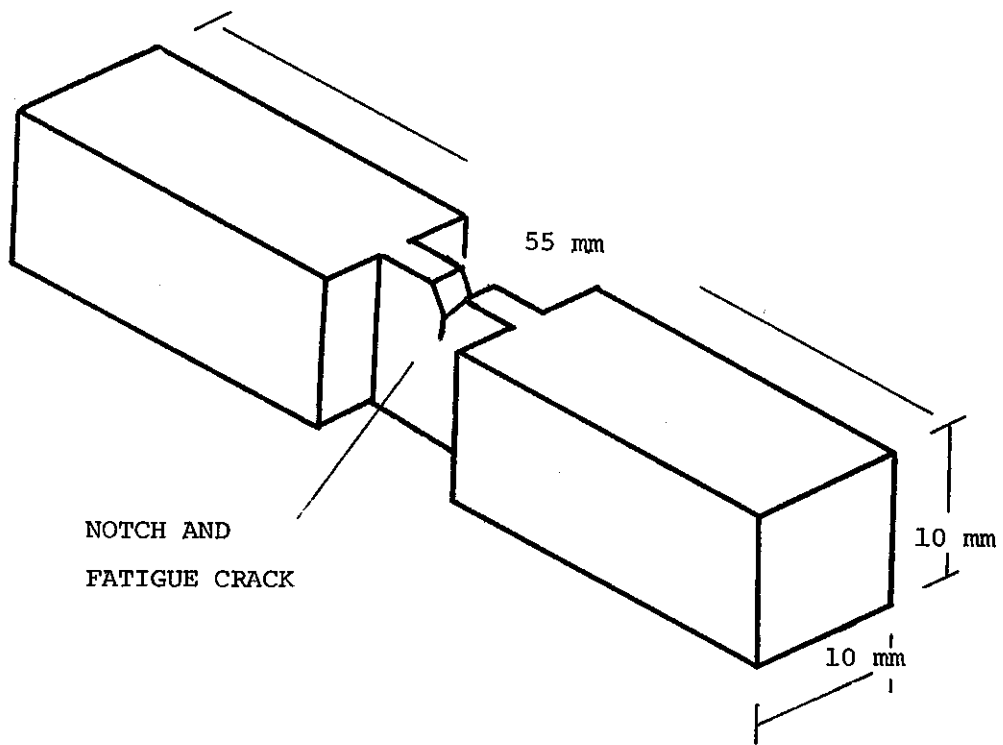


FIGURE 1 FRACTURE TOUGHNESS TEST SPECIMEN

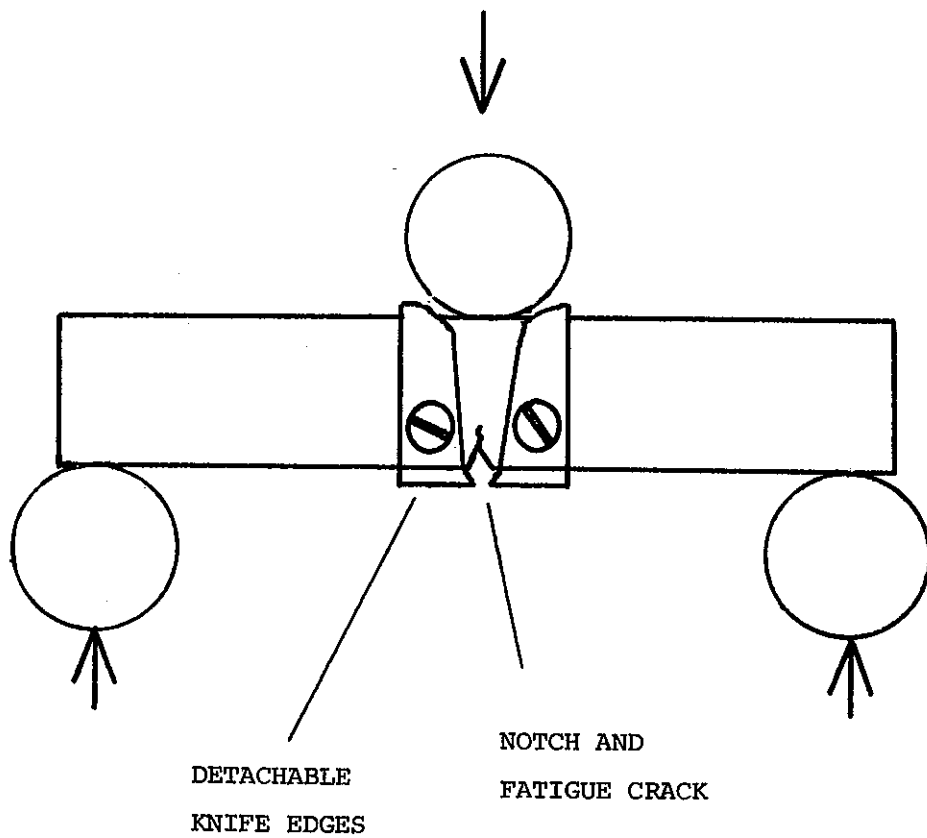


FIGURE 2 LOADING SYSTEM SHOWING DETACHABLE KNIFE EDGES USED TO HOLD THE CLIP GAUGE EXTENSOMETER

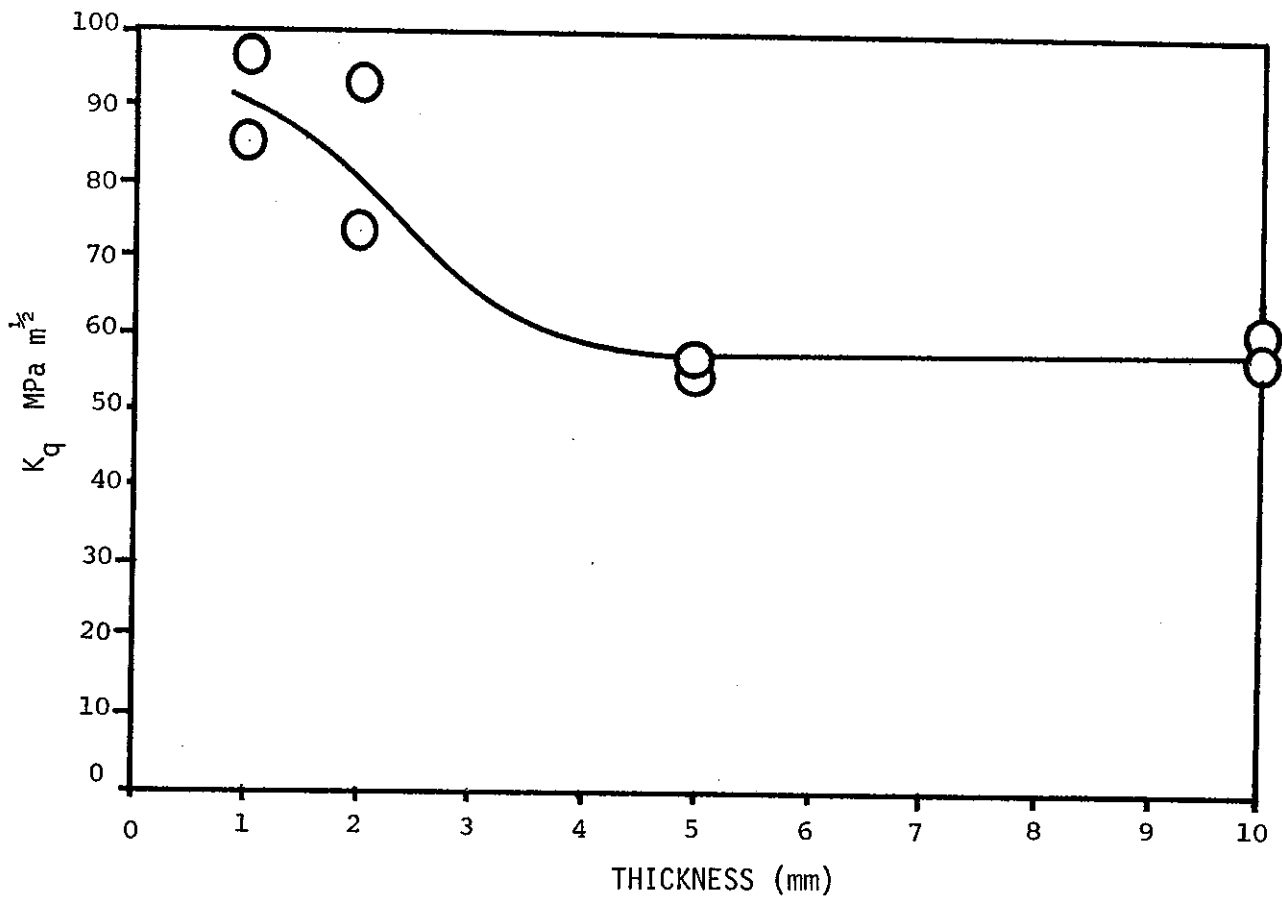


FIGURE 3 PLOT OF FRACTURE TOUGHNESS, K_q , AGAINST SPECIMEN THICKNESS

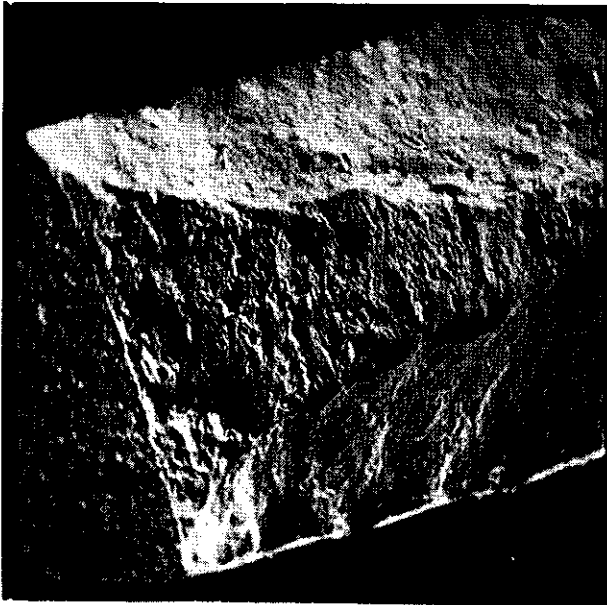


FIGURE 4 SEM FRACTOGRAPH SHOWING OUTER SHEAR LIPS AND CENTRAL PLANE STRAIN REGION ON 1 mm THICK SPECIMEN. FATIGUE CRACK ON LEFT. MAGNIFICATION X 90

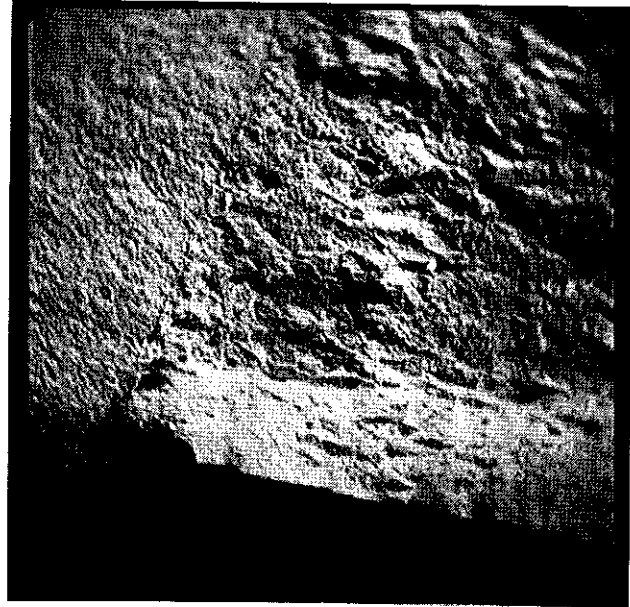


FIGURE 5 SEM FRACTOGRAPH SHOWING SHEAR LIP AT BOTTOM AND FATIGUE CRACK ON LEFT OF 5 mm THICK SPECIMEN. MAGNIFICATION X 60

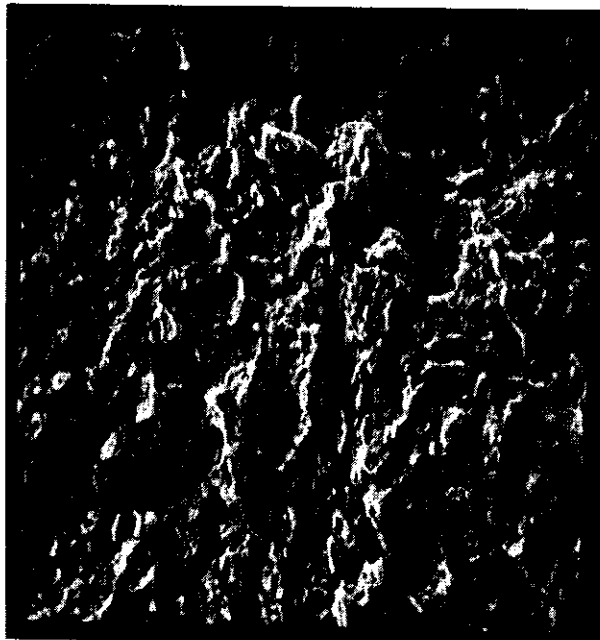


FIGURE 6 SEM FRACTOGRAPH SHOWING DUCTILE NATURE OF CENTRAL PLANE STRAIN REGION OF 5 mm THICK SPECIMEN. MAGNIFICATION X 1000.

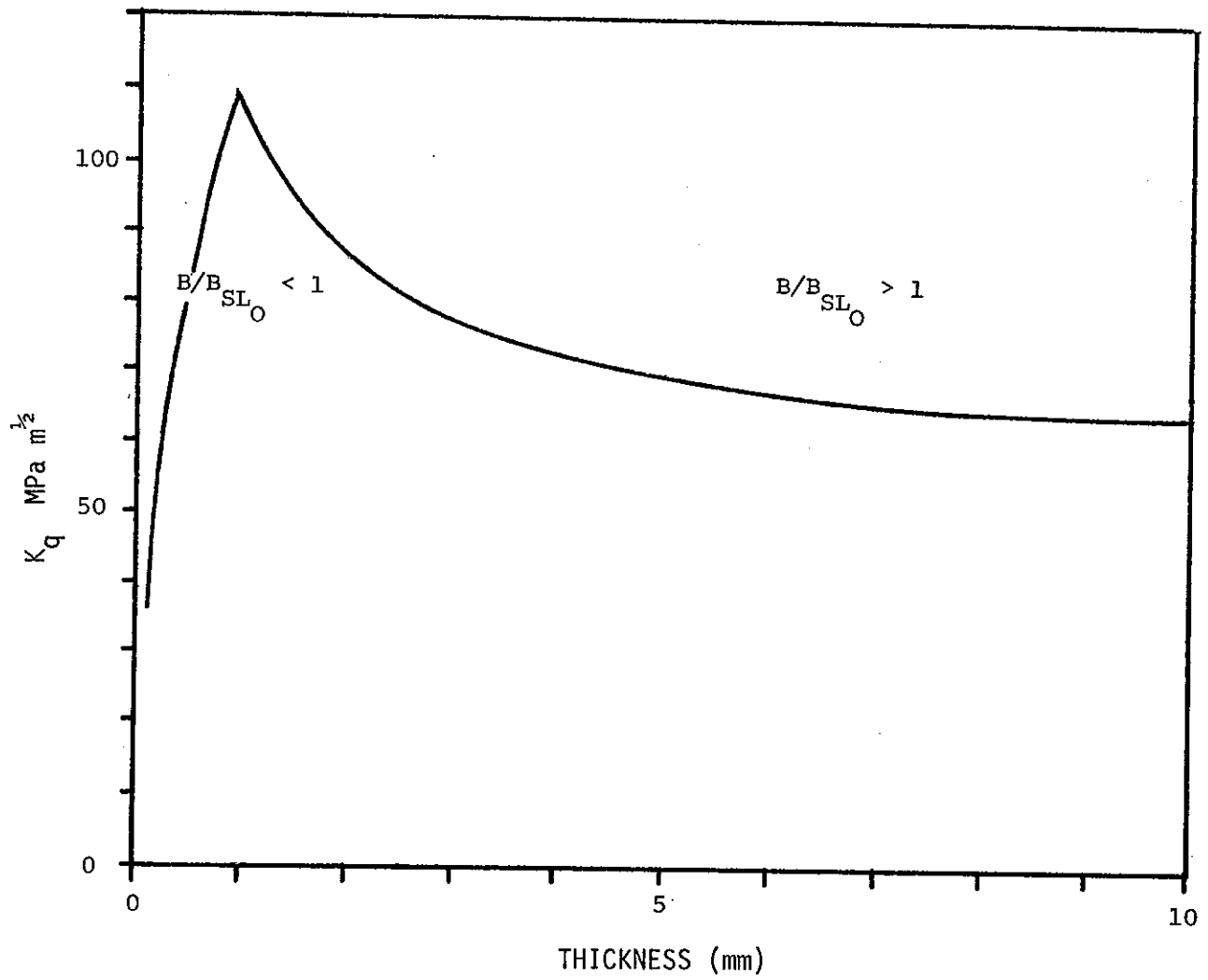


FIGURE 7 VARIATION OF FRACTURE TOUGHNESS WITH SHEET THICKNESS
PREDICTED BY THE MODELS OF BLUHM [1976]

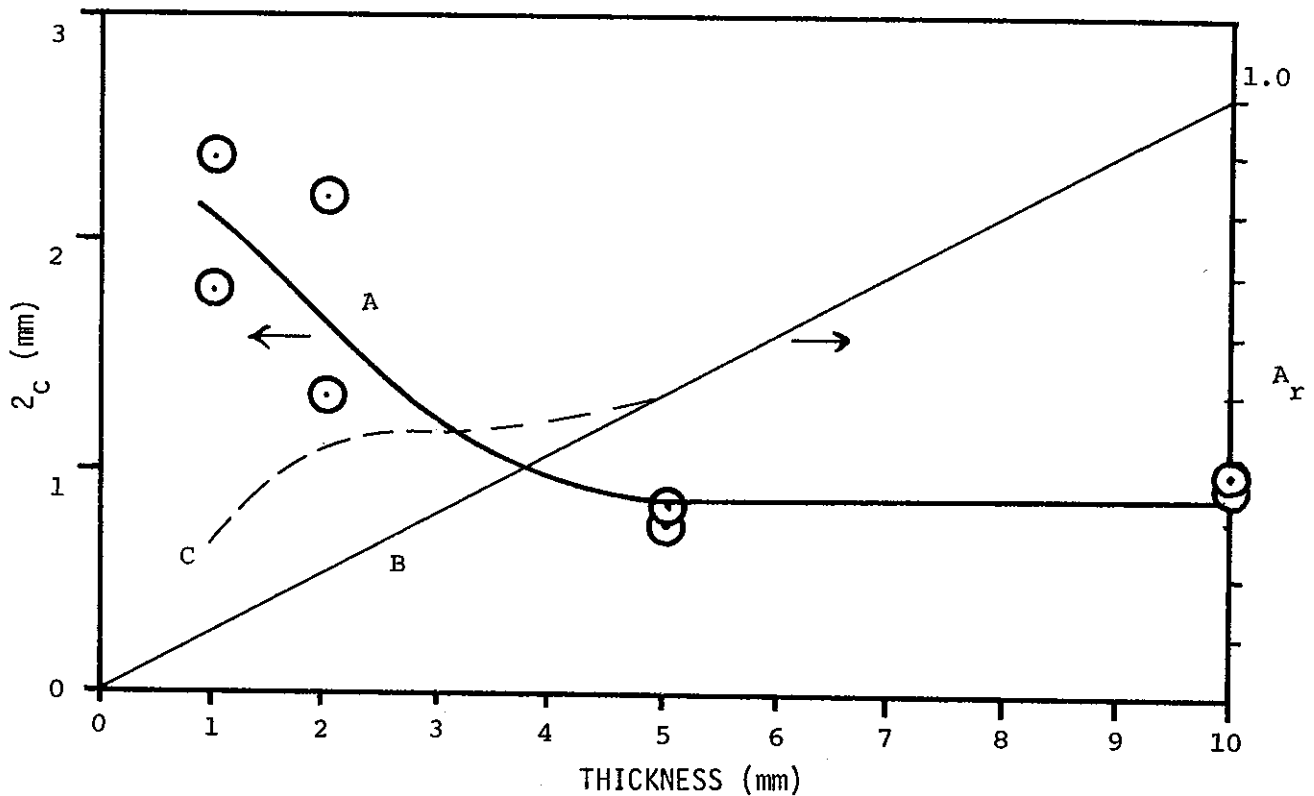


FIGURE 8 CRITICAL FLAW SIZE FOR STRUCTURES OF VARYING THICKNESS
AT A STRESS OF 0.85 OF THE YIELD STRESS

- A. Through-thickness flaws
- B. Relative critical flaw area, A_r , for flaws in material of constant fracture toughness. *Note that for through-thickness rectangular flaws, $A_r = 2c \times t$, and for partial thickness flaws $A_r = 2c \times d$, where t is the wall thickness and d the flaw depth.
- C. As for curve B, but with corrections for the effect of the measured variations in fracture toughness with thickness.

*Flaws falling below curve B are 'safe', flaws above curve B are super-critical.

